

## Interference Structure in the Photoelectron Spectra Obtained from Multiphoton Ionization of $\text{Na}_2$ with a Strong Femtosecond Laser Pulse

Christoph Meier and Volker Engel

Fakultät für Physik, Albert-Ludwigs-Universität, 79104 Freiburg i. Br., Germany  
(Received 20 January 1994; revised manuscript received 5 August 1994)

Kinetic energy distributions of electrons obtained from photoionization of  $\text{Na}_2$  with a femtosecond laser pulse are calculated. Strong pulses induce Rabi oscillations between electronic states of the molecule. The temporal variation of the population in the state which is resonantly coupled to the ionization continuum is transformed into interference patterns in the electron spectra. The situation can be compared to a diffraction experiment where the spatial variation of a grating is reflected in the intensity distribution of scattered particles. It is shown that for short enough pulses the molecule behaves like a three-level system.

PACS numbers: 33.80.Eh, 33.10.-n

Femtosecond experiments investigating the vibrational wave packet motion in the sodium dimer have been performed employing weak [1,2] and strong [3] pulses. Important information about the dynamics of molecular direct ionization and competing ionization mechanisms was obtained. As in other experiments [4], a pump-probe scheme was employed to record the dynamics in several electronic states. In the present study we will concentrate on the information which can be obtained from the measurement of the kinetic energy distribution of photoelectrons produced by a *single* femtosecond laser pulse for different intensities of the pulse. For weak intensities and a pulse of  $\sim 120$  fs duration, the photoelectron time-of-flight spectrum for  $\text{Na}_2$  has already been measured [5]. Also, interesting effects which occur in one-pulse femtosecond experiments on  $\text{H}_2$  [6] and atomic systems [7] have been reported recently. Structures in the photoelectron spectrum resulting from atomic autoionization have also been investigated theoretically [8]. In contrast to an atomic system a diatomic molecule possesses internal degrees of freedom associated with the vibration and rotation of the nuclei. These motions influence the ionization process so that we encounter a more complex situation than in atomic ionization.

We use the same theoretical model which was able to reproduce the results of the  $\text{Na}_2$  experiments [3,9]. Details of the model can be found in the above references. For a molecular beam experiment the initial rotational distribution is cold and the rotational motion of the heavy  $\text{Na}_2$  molecule is essentially frozen on the femtosecond time scale. We thus ignore the rotational degree of freedom in our study. Figure 1 shows the potential curves which participate in the direct photoionization of the molecule if a laser wavelength of  $\sim 625$  nm is used. They belong to the  $X^1\Sigma_g^+$ ,  $A^1\Sigma_u^+$ ,  $2^1\Pi_g$  electronic states of  $\text{Na}_2$  and the  $2^2\Sigma_g^+$  ground state of the ion.

We numerically solve the time-dependent Schrödinger equation for the vibrational wave functions  $\chi_X, \chi_A, \chi_\Pi$ , and  $\chi_I$  in the four electronic states which are coupled by

a laser field. To treat the ionization continuum the total ionic wave function is expanded in terms of electronic eigenstates  $|E\rangle$  containing the core and free electrons. The states are labeled according to the kinetic energy  $E$  of the ejected electrons:

$$|\psi_I(R, t)\rangle = \int_0^\epsilon dE \chi_I(R; E, t) |E\rangle, \quad (1)$$

where  $\epsilon$  is the largest energy which can be transferred to the electron and  $R$  is the internuclear distance.  $\chi_I(R; E, t)$  are the vibrational wave functions of  $\text{Na}_2^+$ , corresponding to the emission of an electron with kinetic energy  $E$ . Instead of discretizing the continuum we expand the functions  $\chi_I(R; E, t)$  in a set of orthogonal polynomials. This leads to a tridiagonal Hamilton matrix which in our case is typically of a dimension of  $100 \times 100$ , including the three neutral states and the ionization continuum. For details of this method see the paper by Seel and Domcke [10] who adopted a method by Burkey and Cantrell [11].

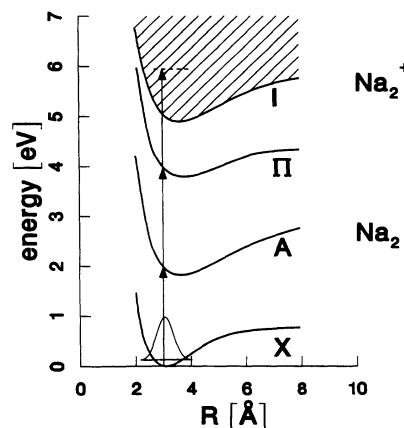


FIG. 1. Potential energy curves of the electronic states which participate in the direct three-photon resonant photoionization of the sodium dimer. The arrows correspond to an excitation energy of 1.98 eV (625 nm).

The laser field of frequency  $\omega$  and field strength  $E_0$  is described as  $f(t)E_0 \cos(\omega t)$ , with  $f(t)$  being the pulse shape which we chose to be a  $\text{sech}^2(t/T)$  function. The time-dependent Schrödinger equation is solved with the condition that the molecule is initially in its electronic and vibrational ground state of energy  $\epsilon_0$ .

From the numerical calculation we obtain the  $\Pi$ -state population as a function of time

$$P_{\Pi}(t) = \int dR |\chi_{\Pi}(R, t)|^2, \quad (2)$$

as well as the electron spectra, defined as

$$P_I(E) = \lim_{t \rightarrow \infty} \int dR |\chi_I(R; E, t)|^2. \quad (3)$$

The transition dipole moments  $\mu_{XA}$  and  $\mu_{A\Pi}$  between the neutral states were taken from Ref. [12]. Employing the Condon approximation, the dipole moments are set to their values at the equilibrium position in the ground state. Since we do not have information about the transition dipole moment  $\mu_{\Pi I}$  between the  $\Pi$  and the ionic state, we have set it to 1/10 of  $\mu_{XA}$ . This is motivated by the fact that, in general, the coupling to the continuum is much smaller than between bound states. We note that changing the magnitude of the moment by a factor of 10 does not alter the results presented below significantly and that the present choice yields theoretical results which are consistent with experimental findings [3]. We furthermore assume the dipole moment to be independent of the electron energy  $E$  [13].

Figure 2 displays the electron spectra calculated within the full quantum mechanical treatment using the four potential curves of Fig. 1 and a 60 fs pulse (FWHM) with intensities of  $0.1I_0$  and  $I_0$  ( $I_0 = 1.86 \times 10^{11}$  W/cm $^2$ ). Also, the time evolution of the population in the  $\Pi$  state

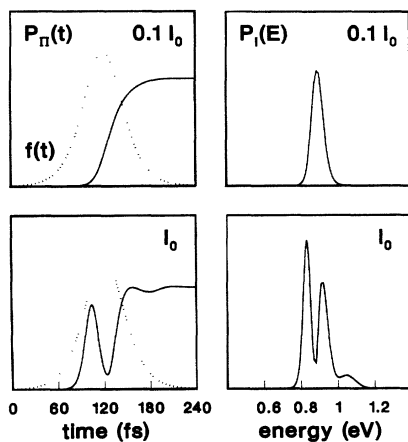


FIG. 2. Left:  $\Pi$ -state population (full line) obtained with two pulse intensities as indicated ( $I_0 = 1.86 \times 10^{11}$  W/cm $^2$ ). The dotted lines show the temporal variation of the envelope function of the laser pulse of width 60 fs. Right: Corresponding photoelectron spectrum calculated within the full quantum mechanical description.

of the molecule is shown. The dotted line is the shape function  $f(t)$  of the pulses. For an intensity of  $0.1I_0$  the electron distribution is a smooth function of energy peaked around 0.9 eV, which simply is  $\epsilon_0 + 3\hbar\omega - V_I(R_0)$ ,  $\hbar\omega$  being the photon energy and  $V_I(R_0)$  the ionization potential at equilibrium distance, as indicated with arrows in Fig. 1.

The appearance of the spectrum changes if the intensity is increased by a factor of 10. In this case the electron spectrum shows a complicated structure. The structure is correlated to the time evolution of the population in the different neutral states. Since the  $\Pi$  state is coupled to the ionization continuum, its population change is, as we will see below, directly connected to the structures in the spectrum. In the present case,  $P_{\Pi}(t)$  does not increase monotonically. The laser-molecule interaction is strong enough to induce Rabi-like oscillations between the electronic states of the molecule.

To understand the complex mechanism of the ionization process one has to keep in mind that a short pulse of 60 fs creates wave packets in the electronic states which are a coherent superposition of the respective vibrational eigenstates. During the field-molecule interaction, the  $\Pi$ -state wave packet moves away from the region, and the electronic states are resonantly coupled by the electric field. This "resonance region"  $\Delta R$  is located around the equilibrium position  $R_0$  in the electronic ground state where  $\hbar\omega$  equals approximately the energy difference between the potentials of the respective electronic states (see Fig. 1). The intensity  $I_0$  is chosen such that a corresponding resonant three-level system, which cannot account for this dynamical effect, would exhibit two population maxima and drop to zero after the pulse has died out. With  $\Omega = (E_0/2)\sqrt{\mu_{XA}^2 + \mu_{A\Pi}^2}$  being the Rabi frequency for a three-level system [14,15] and  $T$  as above, this implies that  $\Omega T = 2\pi$ . Hence the wave packet, escaping the resonance region, prevents the molecule from being depopulated towards the end of the pulse.

The influence of the vibrational dynamics can be eliminated by using even shorter pulses: Fig. 3 shows

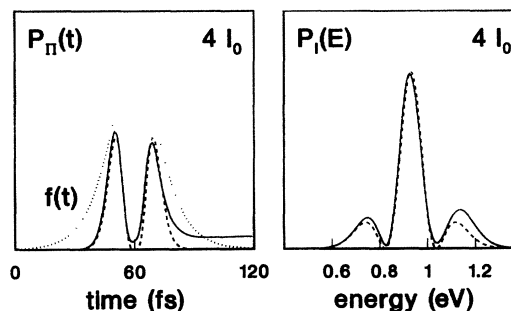


FIG. 3. Same as Fig. 2 but for an intensity of  $4I_0$  ( $I_0 = 1.86 \times 10^{11}$  W/cm $^2$ ) and a pulse width of 30 fs. Additionally, the analytical results for a resonant three-level system are displayed (dashed line).

the same calculation for a pulse of 30 fs FWHM and an intensity of  $4I_0$ , thus keeping the  $\Omega T = 2\pi$  condition unchanged. In this case, the electron spectrum shows a structure somehow reminiscent of the interference pattern of a double slit. We will show that treating the ionization step perturbatively, and neglecting the vibrational motion of the nuclei, the pattern in the electron spectrum can be regarded as an interference effect originating from the two-peak structure of the temporal variation of the  $\Pi$ -state population.

Within first order perturbation theory [16] the nuclear ionic wave function is

$$\chi_I(R; E, t) = \frac{\mu_{\Pi I} E_0}{2i\hbar} \int_0^t dt' \times f(t') e^{-i/\hbar H_I(t-t')} e^{-i(\omega - E/\hbar)t'} \chi_{\Pi}(R, t'), \quad (4)$$

where  $H_I$  denotes the Hamiltonian for the ionic state. Neglecting the vibrational motion means setting the kinetic energy operators in the Hamiltonian to a constant. Since the transition mainly takes place in the resonance region  $\Delta R$  around  $R_0$ , we replace the  $R$  dependence of  $\chi_{\Pi}(R, t)$  and the potentials by the respective values at  $R_0$  and restrict the space integration in Eqs. (2) and (3) to the region  $\Delta R$ . Now the molecular problem is formally equivalent to that of a resonant three-level system which can be solved analytically for a  $\text{sech}^2$  pulse [17]. In Fig. 3 we compare the results of the three-level description (dashed line) with those of our full quantum mechanical calculation (full line). A value of  $\Delta R = 0.2 \text{ \AA}$  was used. The curves agree almost perfectly, however, a small effect due to the nuclear vibrational motion can be seen: The exact population does not drop to zero at the end, as predicted by the simple three-level description.

Within our three-level model the electron spectrum can be seen to be the Fourier transform of the product of the  $\Pi$ -state amplitude  $a_{\Pi}$  with the pulse envelope function  $f(t)$ :

$$P_I(E) = \Delta R \left( \frac{\mu_{\Pi I} E_0}{2\hbar} \right)^2 \left| \int_{-\infty}^{+\infty} dt \times e^{i/\hbar [V_I(R_0) - V_{\Pi}(R_0) - (\hbar\omega - E)]t} f(t) a_{\Pi}(t) \right|^2. \quad (5)$$

Here we have used the interaction representation:  $a_{\Pi}(t) = e^{i/\hbar V_{\Pi}(R_0)t} \chi_{\Pi}(R_0, t)$ . The Fourier transform is to be taken with respect to the difference potential  $V_I - V_{\Pi}$  at the resonance position  $R_0$  minus the energy  $\hbar\omega - E$ . The electron spectrum  $P_I(E)$ , according to Eq. (5), is displayed as a dashed line in Fig. 3, and we find a very good agreement with the results of the full calculation.

If we identify the  $\Pi$ -state amplitude with the aperture function of a diffraction grating and the pulse envelope with its length, it is obvious from (5) that the electron spectra correspond to the pattern seen in a diffraction experiment [18]. That we encounter the particular interference structure in Fig. 3 is due to the fact that in a resonant

three-level system the amplitude  $a_{\Pi}(t)$  is real and does not change its sign [17].

Once the "freezing" of the vibrational motion of the nuclei is established, one can [for the "double-slit-case" (Fig. 3)] obtain the Rabi frequency  $\Omega$  of the system from the interference structure of the photoelectron spectrum. This yields the product of the peak field strength and the averaged dipole moments  $\bar{\mu} = \sqrt{\mu_{AX}^2 + \mu_{A\Pi}^2}$ . The separation of the minima in our calculated electron spectrum is 0.22 eV, which corresponds to a temporal splitting of the population maxima of 19 fs. Using the analytical results for the  $\text{sech}^2$  pulses [17] employed by us, we get a value of 3.8 a.u. for  $\bar{\mu}$ , which is in good agreement with the values of 1.44 and 3.6 a.u. for  $\mu_{AX}$  and  $\mu_{A\Pi}$ , as used in the calculation.

The possibility to measure the diffraction peaks is limited by the resolution of the electron detector. In the present case and for an intensity  $4I_0 = 7.5 \times 10^{11} \text{ W/cm}^2$ , the peak separation is  $\sim 0.2 \text{ eV}$ , which is about a factor of 10 larger than the resolution of a standard electron spectrometer. Thus, the detection of the interference effects should be possible. However, it is necessary to tune the intensity rather smoothly and record different spectra to monitor the change from an unstructured distribution to the case where two or even more peaks can be seen. It is important to keep in mind that for longer pulses the vibrational wave packet dynamics becomes important and the interference structures are washed out. This shows that the effects discussed here can only be measured for molecular systems if pulses much shorter than the vibrational period are employed so that the nuclear motion is frozen during the interaction time. In this case the molecule appears to be similar to a resonant multilevel system. The resolution of the interference structures may also be lowered because of laser focus effects, since molecules being localized in different regions of space experience a different field intensity.

Altogether we have shown that resonant multiphoton ionization with a single femtosecond laser pulse yields electron distributions which show interference patterns. They result from population changes on the femtosecond scale in the electronic state which is resonantly coupled to the ionization continuum. Since the changes are connected to the product of pulse field strength and electric transition dipole moments, it is possible, if the peaks are resolved, to obtain the magnitude of this product from the measurement of the electron kinetic energy distribution for different pulse intensities. This opens the possibility to determine an average value of the moments if the field strength is known or, if the moments are known, to estimate the pulse intensity.

In this Letter we discussed a very general interference effect, and the  $\text{Na}_2$  molecule was used as an example. We would like to emphasize that the participation of other

electronic states in the ionization process, e.g., doubly excited Rydberg states is not unlikely [1,2,5,9]. This might obscure the effect we discussed above.

Experiments on the photoelectron distribution obtained by femtosecond ionization of the sodium dimer have been performed for moderate intensities [5] and are currently repeated for higher intensities [19].

We thank T. Baumert, J. S. Briggs, and G. Gerber for helpful comments. Financial support by the Deutsche Forschungsgemeinschaft within the SFB 276 is acknowledged.

- 
- [1] T. Baumert, M. Grosser, R. Thalweiser, and G. Gerber, *Phys. Rev. Lett.* **67**, 3753 (1991).
- [2] T. Baumert, B. Bühler, M. Grosser, R. Thalweiser, V. Weiss, E. Wiedenmann, and G. Gerber, *J. Phys. Chem.* **95**, 8103 (1991).
- [3] T. Baumert, V. Engel, Ch. Meier, and G. Gerber, *Chem. Phys. Lett.* **200**, 488 (1992).
- [4] L. R. Khundkar and A. H. Zewail, *Annu. Rev. Phys. Chem.* **41**, 15 (1990); A. H. Zewail, *Farad. Discuss. Chem. Soc.* **91**, 207 (1991); A. H. Zewail, *J. Phys. Chem.* **97**, 12427 (1993).
- [5] T. Baumert, B. Bühler, R. Thalweiser, and G. Gerber, *Phys. Rev. Lett.* **64**, 733 (1990).
- [6] P. H. Bucksbaum and A. Zavriyev, in *Coherence Phenomena in Atoms and Molecules in Laser Fields*, edited by A. D. Bandrauk and S. C. Wallace, NATO ASI, Ser. B Physics, Vol. **287** (Plenum Press, New York, 1992).
- [7] W. Nicklich, H. Kumpfmüller, H. Walther, X. Tang, Huale Xu, and P. Lambropoulos, *Phys. Rev. Lett.* **69**, 3455 (1992).
- [8] K. Rzażewski, *Phys. Rev. A* **28**, 2565 (1983); J. W. Haus, M. Lewenstein, and K. Rzażewski, *J. Opt. Soc. Am. B* **1**, 641 (1984).
- [9] V. Engel, T. Baumert, Ch. Meier, and G. Gerber, *Z. Phys. D* **28**, 37 (1993).
- [10] M. Seel and W. Domcke, *J. Chem. Phys.* **95**, 7806 (1991).
- [11] R. S. Burkey and C. D. Cantrell, *J. Opt. Soc. Am. B* **1**, 169 (1984); **2**, 451 (1985).
- [12] D. D. Konowalow, M. E. Rosenkranz, and D. S. Hochhauser, *J. Mol. Spectrosc.* **99**, 321 (1983).
- [13] W. Chupka, in *Ion-Molecule Reactions*, edited by J. L. Franklin (Butterworths, London, 1972), Vol. 1.
- [14] G. W. Coulson and K. Bergmann, *J. Chem. Phys.* **96**, 3467 (1992).
- [15] M. H. Mittlemann, *Theory of Laser-Atom Interaction* (Plenum Press, New York, 1993).
- [16] R. Loudon, *The Quantum Theory of Light* (Clarendon Press, Oxford, 1983).
- [17] C. Meier and V. Engel (to be published).
- [18] K. Iizuka, *Engineering Optics* (Springer, New York, 1987), 2nd ed.
- [19] G. Gerber (private communication).